International Journal of Mechatronics and Manufacturing Systems

ISSN online: 1753-1047 - ISSN print: 1753-1039
https://www.inderscience.com/ijmms

Neural network as approach for detection of non-compliant semi-finished additive manufactured parts

Gianluca D'Urso, Mariangela Quarto

DOI: 10.1504/IJMMS.2023.10057694

Article History:

Received:	09 February 2023
Last revised:	26 April 2023
Accepted:	17 May 2023
Published online:	14 September 2023

Neural network as approach for detection of non-compliant semi-finished additive manufactured parts

Gianluca D'Urso* and Mariangela Quarto

Department of Management, Information and Production Engineering,
University of Bergamo,
Via Pasubio7/b, 24044, Dalmine (Bergamo), Italy
Email: mariangela.quarto@unibg.it
Email: gianluca.d-urso@unibg.it
*Corresponding author

Abstract: The integration of artificial intelligence and algorithms for the elaboration of data with the new advanced technologies represents an interesting topic for the definition of reliability and repeatability of the process. The present work combines these elements for improving the process chain of metal-material extrusion (metal-MEX), developing an algorithm able to predict which parts will be non-compliant after the debinding and sintering processes necessary for obtaining the final parts. Specifically, considering a database containing historical data collected by the authors in their previous research, an artificial neural network (ANN) was trained to be applied immediately after the printing stage for detecting non-compliant parts. In this way, it is possible to avoid the post-printing treatment (debinding and sintering) for parts that do not respect the design requirements. Considering the validation of the model, the ANN can discriminate which parts will be able to satisfy the requirements, supporting the operator in the selection of compliant and non-compliant parts.

Keywords: geometrical accuracy; prediction; additive manufacturing; ANN; artificial neural network; quality assessment; non-compliant detection.

Reference to this paper should be made as follows: D'Urso, G. and Quarto, M. (2023) 'Neural network as approach for detection of non-compliant semi-finished additive manufactured parts', *Int. J. Mechatronics and Manufacturing Systems*, Vol. 16, Nos. 2/3, pp.261–279.

Biographical notes: Gianluca D'Urso is a Full Professor and Deputy Director of the Department of Management, Information and Production Engineering, University of Bergamo. He is Rector's delegate for applied research. His research interests include forming technologies, friction stir welding, micro-manufacturing with a particular focus on micro-EDM process, discrete event and finite element simulation and during last year also additive manufacturing processes.

Mariangela Quarto is a researcher of the Department of Management, Information and Production Engineering, University of Bergamo. She received her PhD in Economic and Management of Technology from University of Pavia. Her research interests include micro-EDM, optimisation processes from economical and technical point of view through the application of models and algorithms and additive manufacturing processes.

1 Introduction

Additive manufacturing (AM) was born in the 1980s and has mostly been used for Rapid Prototyping since then (Kruth et al., 1998; Levy et al., 2003). Further developments turned the processes into a technology capable of production (Levy et al., 2003), up to being used for additive manufacturing of end-use parts, known as Rapid Manufacturing (Lieneke et al., 2016) for applications in various fields such as mechanical engineering, medicine, fashion and art (Wohlers et al., 2021). Compared with traditional processes, AM processes create products of different materials through the successive deposition of layers.

In recent years, the industrial world has been focusing on AM as a key factor in a new revolution in industrial manufacturing systems (Ferreira et al., 2004; Sun et al., 2005). Due to this development, the application and the interest in these technologies increase allowing the technology development and the increment in the printable materials. Precisely the introduction of AM technologies in the world of metals has meant that many of the theoretic hypotheses and problems are found to be real. The development and application of these processes in real cases and/or in laboratories have led not only to many opportunities but also to several criticalities (Fera et al., 2016).

Additive manufacturing can offer many benefits over the use of formative tools, specifically, it provides new opportunities thanks to the great design freedoms, such as complex lattice structures or helical cooling channels; at the same time, new technical and economic advantages can be highlighted. For example, it is possible to reduce the time-to-market of new products since the design phase and the activity for preparing the machine are faster compared with traditional processes. From the economic point of view, it is possible to decouple production costs and part complexity (Quarto and Giardini, 2022), allowing the demand for these processes to increase (López Rojas et al., 2022). Indeed, AM processes result to be convenient just for low production volume, since this kind of process is completely free from the economy of scale (Quarto and Giardini, 2022).

Despite these benefits, the usage of additive manufacturing for end-use part production is still limited (Ryan et al., 2021). Different process-specific challenges such as rough surfaces or the stair-stepping effect caused by layer-by-layer manufacturing harm the industrial establishment. Furthermore, end-use part production requires accurate knowledge and understanding of all restrictions and possibilities (Wiberg et al., 2019). Therefore, manufacturing design restrictions have been the subject of numerous studies (Wiberg et al., 2019; Giudice et al., 2021; Giganto et al., 2022). Geometrical accuracy is another very important aspect requiring further determinations and improvements (Al-Ahmari et al., 2019; Liravi et al., 2015). However, these issues inhibit the use of additive manufacturing in Rapid Manufacturing and Rapid Tooling. Such deviations are insufficiently studied (Wohlers et al., 2021), although, the literature demonstrates that various research was performed to classify the geometrical accuracy of additive manufacturing (Gregorian et al., 2001; Byun and Lee, 2003; Boschetto and Bottini, 2014; Brøtan, 2014). Specifically, most of the references evaluate the geometrical accuracy with standard benchmark parts and this is not enough since several geometrical factors affect the geometrical accuracy. Additionally, the derivation of tolerances is often lacking and reasons for the occurrence of dimensional deviations are often unknown. As a result, there is a knowledge gap regarding achievable tolerance values for the actual limitation

of geometrical deviations (Wohlers et al., 2021). Additionally, the effect of printing parameters on geometrical accuracy has been poorly studied (Lieneke et al., 2020).

Nowadays, the change in production techniques due to Industry 4.0 has increased the impact of digitisation on products. Replacing the operator with statistical algorithms for error detection in production processes is becoming increasingly common, introducing new solutions based on the huge amount of data collected by systems. This process can be defined as Quality 4.0: the digitalisation of total quality management (TQM) that impacts the quality of technologies, processes, and resources (physical and human). Predictive quality is one of the widely applied quality solutions specifically applied to avoid unnecessary waste of time and effort to prevent and predict quality problems in products and processes. Quality problems are defined as all those situations that reduce performance levels or cause many wastes as a result of product recalls because of defects. The introduction of a predictive quality system evaluation is focused on the reduction of product recalls and it aims to achieve zero-defect production. This results in higher quality and thus a higher degree of customer satisfaction (Yorulmuş et al., 2022).

Different researchers focused their attention on the development of new algorithms and approaches based on machine learning and artificial intelligence for optimising process parameters, predicting part properties, and detecting and classifying the products/processes defects (Czimmermann et al., 2020; Chen et al., 2021; Meng et al., 2020). While these techniques have been developing for several decades, their applications in the AM field are only several years old. Researchers developed different methods and approaches, firstly for learning the relevance of the relationship between the processing parameters and property using existing data to guide for optimising these processing parameters. Secondly, these models can predict the geometric deviation based on the designed geometry and guide the compensation. Thirdly, these approaches are good at dealing with in situ images and acoustic emissions during printing and detecting defect formation in real time (Meng et al., 2020).

ANN surely are one of the most common techniques applied to different processes and with different aims. For example, a combination of thermographic off-axis imaging as data source and deep learning-based neural network architectures to detect printing defects were developed in Baumgartl et al. (2020), obtaining accuracy in the prediction of 96.80%. Similarly, in Papazetis and Vosniakos (2019) a highly reliable ANN was constructed and trained to predict shape fidelity and material flow rate in the material extrusion process. In Westphal and Seitz (2021), the convolutional neural network was applied for detecting the surface defects. Yadav et al. (2020) combined the artificial neural network (ANN) with the genetic algorithm creating a supporting tool for the definition of the printing parameters able to improve the mechanical characteristics. Different approaches were compared to determine the most appropriate method for the investigation of the process accuracy showing a percentage of reliability in a range between 82.5% and 92% (Kordatos and Benardos, 2022).

ANN is applied also in different machining processes such as friction stir welding (Quarto et al., 2022a) and micro-electrical discharge machining (Quarto et al., 2022b) combined with Finite Element Method and particle swarm optimisation respectively, demonstrating the ANN flexibility and ability to be integrated with different methods. All these aspects help to improve specific elements of the processes, but considering industrial digitisation in its entirety, in the future they can be integrated helping the definitions of the logic behind the digital twin (Jarosz and Özel, 2022; Ibrahim et al., 2020).

The present publication focuses on Material Extrusion (MEX), an extrusion process using a thermoplastic filament which is melted, extruded, and filed on the substrate (*x-y* plane) by a heated nozzle. After the completion of each layer, the build platform (or the nozzle, which is related to the machine movement) is lowered in the z-direction (or raised) to create space for the next layer (Wohlers et al., 2021; International Organization for Standarization, 2021; Fischer et al., 2014). The thermoplastic filament is made up of metal powder dispersed into a polymeric matrix (Quarto et al., 2021; Carminati et al., 2022). This process differs from the MEX of polymers since the product coming from the printing activity (called green part) is composed of both metal and polymer. Subsequently, the green parts (*GP*) undergo debinding and sintering treatments for removing the polymeric components, thus obtaining the white part (*WP*): a metallic component. Given this process chain, without the introduction of intermediate quality assessment systems, the certainty that the white part respects the required geometric and dimensional characteristics is obtained only at the end of the entire process. This means that if a part does not meet the requirements it is discarded after the entire production process, wasting time, materials, and resources. This work aims to introduce a quality assessment immediately after the printing phase (Figure 1). This assessment would be based on the development of an algorithm defined by a trained ANN able to predict the white part geometric and dimensional characteristics, by exploiting the information derived from measuring the green part.

Figure 1 General new process chain (see online version for colours)

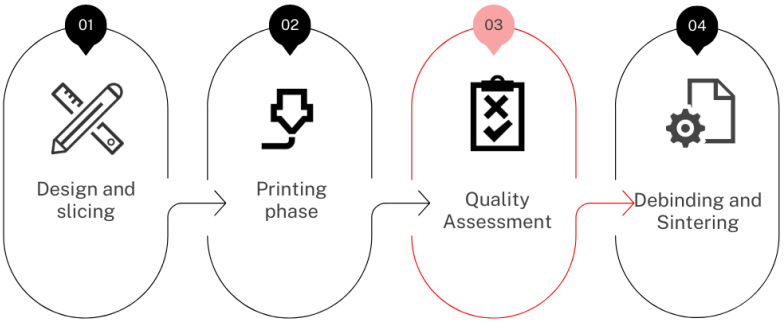

To the best of the authors' knowledge, the real novelty of this work is related to the position of the quality assessment. Today, it is placed at the end of the process chain evaluating the final dimension and geometrical characteristics directly of the white part. Through the developed approach it is possible to anticipate this evaluation and avoid the treatment of non-compliant parts. Furthermore, this approach is able to show compliance with various requirements at the same time and it is adaptable as a function of the company/operator's needs.

2 Problem formulation

A metal-Material Extrusion (metal-MEX) is an Additive Manufacturing process performed by extruding a filament made up of metal powder, equally distributed in a polymeric matrix. Once the printed part, called Green Part (*GP*), is undergoing the

debinding and sintering processes, the final part (white part – *WP*) undergoes a dimensional shrinkage, which makes it necessary to oversize the parts in the design phase. Therefore, the general process does not allow knowing the final characteristics of the part before the post-printing processes. This means that time and money are wasted and the only solution for respecting the necessary production volume is to forecast an increment in the printing process as a function of process capability and defects history.

To overcome or reduce the impact of printing defects, the concept of Quality 4.0 integrated with artificial intelligence can be implemented in the system. Thus, an algorithm able to predict the characteristics of the product in the middle of the process chain can improve the system efficiency reducing the waste of time and material. The waste of time would be reduced because the identification of the non-compliant parts would be anticipated. The waste of material would be reduced because the discarded parts (green parts) may be reintroduced into the process cycle, for example creating a new filament, so reducing the waste of material. The idea of the process generated by introducing this algorithm for detecting non-compliant parts before the end of the process chain is illustrated in Figure 2.

Figure 2 Process flow (see online version for colours)

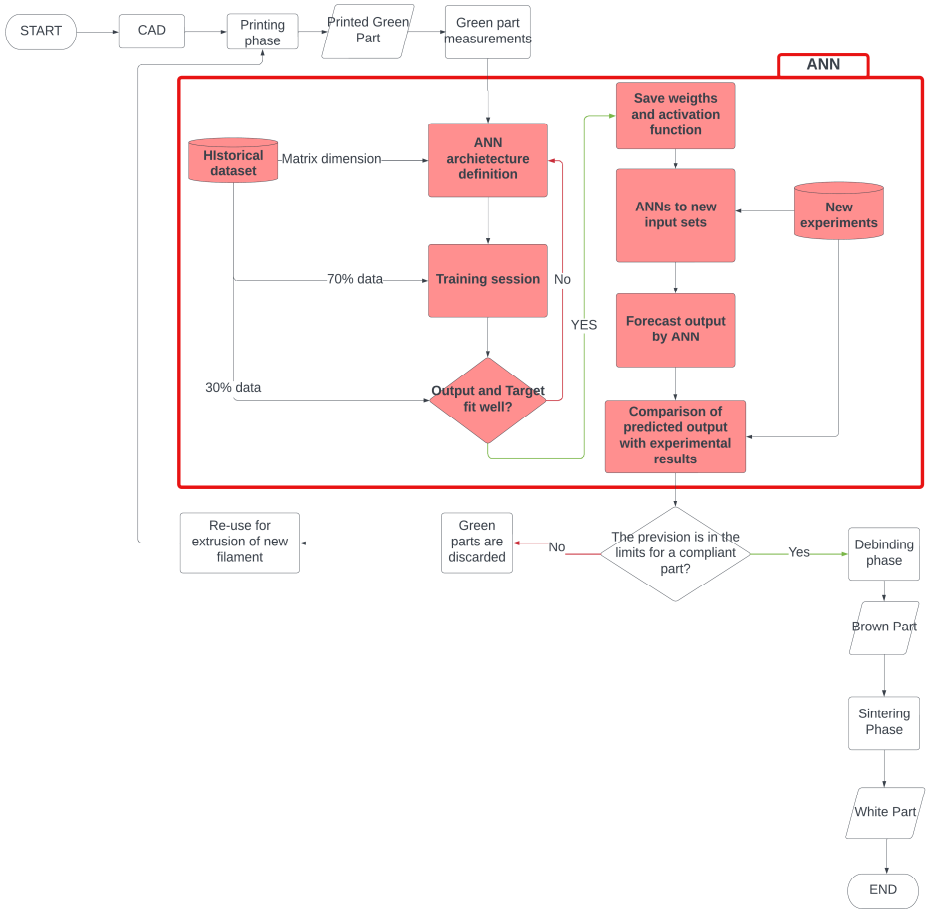

3 Materials and methods

3.1 Equipment and material

The metal-MEX process can be divided into two main stages. The first stage includes all the activities necessary for setting up the equipment and the actual production of the designed parts. The testing samples were fabricated using a MEX polymeric machine, Ultimaker 5S, equipped with a direct drive extruder with a hardened steel nozzle CC0.6 of diameter 0.6 mm, which was the smallest nozzle diameter, limiting the clogging problem. A filament with a diameter of 2.85 mm, provided by BASF (Ultrafuse 316L), was used. This is an innovative filament that is made up of 316L austenitic stainless-steel powders (90 wt%), evenly distributed in a polymeric matrix composed of polyoxymethylene (POM) and polyolefin. The immobilisation of the metal particles and the uniform distribution of the metal within the binder matrix allow for safe and simple handling. The parts are built up layer upon layer from a mouldable material, with the polymer content of the filament acting as a binder.

The second stage is related to the debinding and sintering processes. The main polymer content (primary binder) was removed from the so-called green part through a catalytic and thermal debinding process at 120°C with HNO_3 (concentration 98%). The result of this process is the brown part, which consists of pure metal particles and a residual binder (secondary binder). The brown part is characterised by the same volume and a loss of mass compared to the green part. The subsequent sintering process removes the secondary binder from the as-built part and causes metal particle coalescence. The sintering cycle was performed in an argon atmosphere and consisted of three thermal ramps:

- room temperature – 5 °C/min – 600°C, holding time 1 h
- 600°C – 5°C/min – 1380°C, holding time 3 h
- 1380°C – furnace cooling – room temperature.

Considering the previous studies (Quarto et al., 2021; Carminati et al., 2022), this process generates a shrinkage along different directions in a range between 16% (x and y directions) and 20% (z direction). This causes the necessity of oversizing the designed parts and the dimensional control not only at the end of the printing stage but especially after the debinding and sintering processes.

3.2 ANN architecture definition

ANN is a mathematical model able to simulate the capabilities of the human brain. The base learning approach is focused on past activities; in fact, ANN learns from previous experiences how to solve non-linear problems. The general architecture is represented by several layers containing a certain number of nodes called neurons; specifically, these layers are divided into an input layer, an output layer and one or more hidden layers.

The input layer size (input neurons – *IN*) is described by the input matrix. This information is sent from the IN to the hidden layers by means of the activation function, then the elaborated information reaches the output nodes (*ON*). Backpropagation is the most common training, and then a new group of data is used for the tests and validation,

which are conducted for defining the validity and reliability of the net comparing predicting output and targets.

In this case, the main printing parameters (printing temperature, printing speed, layer thickness, infill type) were used as input and as anticipated in the previous section, the main dimensions, and geometrical characteristics of the green part (*GP*) were measured (Table 1). This second group of inputs are very variable since can be changed as a function of what the authors want to evaluate on the white part (*WP*). The *ON* is represented by the geometrical characteristics and dimensions defined as representative of product quality based on the project specifications. Table 1 reports the details about the input and output layers composition used for validating the approach.

Table 1 Summary of input and output nodes

Inputs (IN)		*Outputs (ON)*	
Printing temperature	T	Density WP	δ_{WP}
Printing speed	s	Planarity xy WP	XY_{WP}
Layer thickness	h	Planarity yz WP	YZ_{WP}
Infill	In	Shrinkage x/y WP	S_{WP}
Volume GP	V_{GP}	Shrinkage z WP	Sz_{WP}
Weight GP	W_{GP}		
Planarity xy GP	XY_{GP}		
Planarity yz GP	YZ_{GP}		
Dimension A GP	A_{GP}		
Dimension B GP	B_{GP}		

The sizing of the hidden layer is the most challenging activity in the definition of ANN architecture. Kolmogorov's Theorem was used for demonstrating that a network characterised by a single hidden layer is reliable enough to compute arbitrary decisions; indeed, studies, based on empirical tests using a backpropagation algorithm, demonstrated that no significant advantages are provided by using two hidden layers in comparison to a single one (Hecht-Nielsen and Kolmogorov, 1987; Lippmann, 1987; Cybenko, 1988, 1989; Bounds et al., 1988). Because of these studies, a single hidden layer structure is chosen and then the number of hidden nodes (*HN*) was defined. Such as for the hidden layers, also the sizing of the number of nodes is very important for assuring a proper level of accuracy in the predictions: too many/few neurons can generate overfitting/underfitting situations. Thus, the best architecture is defined by selecting a range in which *HN* can vary during the iterative process able to estimate the prediction error. This means that *HN* is varied through the minimum and maximum values identified by some heuristic methods. Specifically, the lower threshold is heuristically defined according to the literature (Garcia-Romeu et al., 2010; Maren et al., 1990; Majumder et al., 2014) as reported in equation (1).

$$MTI = \frac{IN + ON}{2} \tag{1}$$

The maximum number of *HN* tested is selected defining the maximum value assumed by the Heuristic methods reported below.

- Kolmogorov in Hecht-Nielsen and Kolmogorov (1987), equation (2):

$$KOL = 2IN + 1 \tag{2}$$

- Lippmann in Lippmann (1987), equation (3):

$$LIP = ON(IN + 1) \tag{3}$$

- Kudrycky in Maren et al. (1990), equation (4):

$$KUN = 3 \cdot ON \tag{4}$$

The architecture is defined by iterative training considering $MTI \leq HN \leq \max(KOL; LIP; KUN)$. A Matlab code is written for testing ANN performance.

The training is carried out using the same dataset for all iterations (e.g., input and output values) and calculating the error between the targets and output values. Where the targets represent the output values included in the dataset, while the outputs indicate the predictions. Since the outputs are characterised by different magnitude orders and units of measure, the coefficient of variation (CV_i), a statistical indicator independent from the distribution, is introduced.

Unlike the root mean square error (*RMSE*), *CV* is represented by a pure number. It measures the data dispersion in relation to the average value of the distribution. In this case, it is used for comparing the error of distribution that otherwise could not be compared. CV_i, where *i* indicates the output, is defined as the ratio between the standard deviation of $RMSE_i$ (σ_{RMSEi}) and the average value of the $RMSE_i$ distribution (μ_{RMSEi}) multiplied by 100 (equation (5)).

$$CV_i = \frac{\sigma_{RMSE_i}}{\mu_{RMSE_i}} \cdot 100 \tag{5}$$

where the root mean square error (*RMSEi*) is calculated as follows:

$$RMSE_i = \sqrt{\frac{\sum_{k=1}^{n} (Target_{i,k} - Output_{i,k})^2}{n}} \tag{6}$$

where *k* indicates the sample considered.

For each iteration, the sum of CV_i of each output is defining the CV_{tot}. The minimum value achieved by CV_{tot} identifies the architecture that generates the lowest prediction error. Table 2 reports the value of *CV* estimated during the training phase highlighting the best configuration of the ANN. It is possible to observe that, in this case, the lower CV_{tot} corresponds to the sum of lower CV_i. Such as reported in Figure 3, the final ANN architecture is defined by 10 input nodes identified by the first column of Table 1, 15 hidden nodes distributed in a single layer and 5 output.

Table 2 Summary of estimated CVtot (see online version for colours)

HN	$CV\ \delta_{WP}$	$CV\ XY_{WP}$	$CV\ YZ_{WP}$	$CV\ S_{WP}$	$CV\ Sz_{WP}$	CV_{tot}
8	1.628	1.586	3.107	4.969	9.128	20.419
9	1.637	3.235	5.304	6.198	8.597	24.971
10	1.681	2.226	6.039	3.603	6.992	20.541
11	1.651	3.555	3.901	4.378	8.464	21.563
12	1.803	3.274	3.866	5.527	9.127	23.596
13	2.849	3.516	6.532	7.350	12.572	32.819
14	4.059	6.531	6.747	15.516	15.318	48.170
15	1.318	1.317	2.940	3.406	3.858	12.840
16	1.909	1.950	2.946	4.556	6.584	17.944
17	2.419	3.031	4.301	4.653	5.910	20.313
18	1.827	3.138	4.422	5.040	7.133	21.560
19	2.649	1.532	5.242	7.008	5.645	22.076
20	1.987	3.633	3.290	4.375	5.136	18.421
21	2.317	2.501	4.946	4.387	4.829	18.979
22	1.597	1.632	3.093	6.780	8.627	21.729
23	1.558	2.233	5.173	4.544	4.512	18.020
24	1.649	2.784	4.227	3.588	6.811	19.059
25	1.392	1.944	2.954	6.009	7.149	19.448
26	1.857	2.394	4.281	3.449	3.934	15.916
27	1.725	2.430	5.730	4.622	7.261	21.768
28	2.180	2.262	5.984	5.306	5.653	21.384
29	1.957	5.214	5.812	6.704	8.453	28.139
30	3.106	3.458	4.058	5.460	10.647	26.729
31	2.732	2.945	5.342	3.613	4.734	19.366
32	1.518	3.910	6.507	6.400	8.701	27.038
33	2.664	5.825	5.119	4.863	7.318	25.789
34	2.131	3.358	4.195	3.475	6.406	19.566
35	2.296	7.509	3.685	8.211	13.110	34.811
36	3.633	4.156	6.251	4.568	6.083	24.691
37	1.914	3.596	4.590	10.650	9.943	30.693
38	3.471	1.977	4.906	3.476	9.721	23.552
39	4.654	4.388	6.331	4.413	8.419	28.204
40	2.325	6.883	6.042	17.698	32.048	64.996
41	4.119	3.084	6.233	3.442	3.864	20.741
42	1.515	4.988	5.122	3.474	3.907	19.007
43	2.795	4.815	4.311	3.988	7.454	23.363
44	2.940	5.612	4.474	8.609	13.535	35.169

Table 2 Summary of estimated CVtot (see online version for colours) (continued)

HN	*CV* δ_{WP}	*CV XY*$_{WP}$	*CV YZ*$_{WP}$	*CV S*$_{WP}$	*CV Sz*$_{WP}$	CV_{tot}
45	1.641	4.236	4.195	3.585	3.886	17.543
46	2.989	2.704	5.191	3.608	3.927	18.419
47	3.552	3.877	4.845	11.412	11.188	34.874
48	2.843	9.296	7.237	9.164	11.435	39.976
49	1.947	5.954	4.890	10.906	9.197	32.893
50	2.464	3.217	4.938	3.565	3.896	18.080
51	2.648	3.924	4.085	4.918	6.294	21.869
52	2.030	2.323	7.313	4.143	5.744	21.552
53	3.116	2.479	5.605	3.519	6.277	20.996
54	3.022	7.095	5.635	4.595	11.687	32.034
55	2.412	3.902	4.306	9.270	10.014	29.903

Figure 3 ANN architecture (see online version for colours)

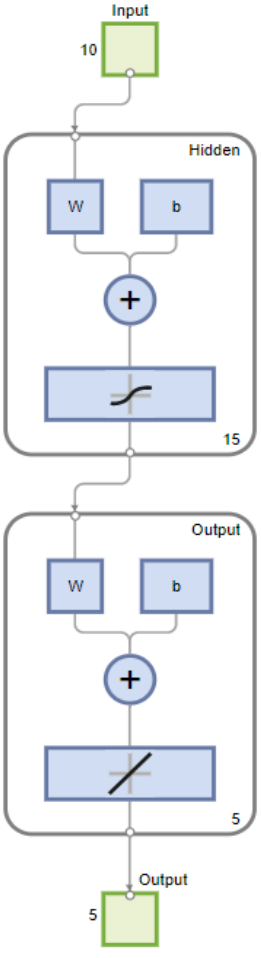

3.3 Training, validation, and test of the ANN

MATLAB tools and code are used. The data contained in the dataset are collected during the use of the material extrusion machine Ultimaker 5S considering different printing parameters. Specifically, the training dataset is composed of historical data collected from printing parts with a different set of printing parameters (Quarto et al., 2021; Carminati et al., 2022) and these data covers a wide range of input combinations for printing different geometries and evaluating different dimensions and geometrical characteristics. A coordinate measurements machine (CMM, Zeiss O-Inspect) using a touching probe having a diameter of 3 mm was used for collecting the necessary measurements, both on *GP* and *WP*. The CMM is able to calculate the distance between the reconstructed plans and the sample volume, furthermore, as a function of the reconstructed profile and geometrical elements, it can extrapolate geometrical characteristics like circularity, flatness, and orthogonality. This approach is used for collecting information about $V_{GP,}$ $XY_{GP,}$ $YZ_{GP,}$ $A_{GP,}$ B_{GP}, $XY_{\mathrm{WP},}$ YZ_{WP}. The shrinkages are calculated as the difference between the measures collected on the green part and the white part related to the green part measure. Their predictions allow estimating different dimensions obtained in the *WP*. The weight is estimated through an analytical scale.

70% of the entire dataset (1188 cases) was used for the training activity through a Levenberg-Marquadrat optimisation algorithm, while the validation and test stages each exploited 15% of the available data. The division is randomly conducted. The dataset allows considering valid the ANN for an interval of printing parameters that include the greater part of printing parameters combination that generate satisfying results (concerning the considered material). Indeed, the trained ANN cover the range of a nozzle temperature between 170°C and 240°C, printing speed between 20 mm/s and 50 mm/s, the main infill path (line, walls..), and layer height between 0.1 mm and 0.4 mm.

The validation of the approach is performed considering a completely new group of samples able to cover part of the trained interval. The benchmark geometry used for the final validation is a cube that, as a white part, should be characterised by $15 \times 15 \times 15$ mm. Due to the shrinkage typical of this process chain defined by a previous study, the nominal dimensions are oversized ($17.4 \times 17.4 \times 18$ mm) considering the shrinkage percentage defined in the previous study (Quarto et al., 2021). The parts are printed applying the combination of printing parameters reported in Table 3, considering 4 repetitions for each combination to evaluate the stability and repeatability of the approach. The material used is a metal-polymer matrix filament Ultrafuse 316L stainless steel. After the printing process, the *GPs* are measured as reported in the previous paragraph for obtaining the necessary input information. Then, all samples were subjected to the sintering and debinding process performed by a third party. In the meantime, the ANN elaborate the data supplying its prediction. Once the white parts are ready, the measurements are conducted for estimating the real shrinkages and density, necessary for the comparison with the predicted results.

Table 3 Printing parameters applied for validation tests

Validation test	*T* (°C)	*S* (mm/s)	*H* (mm)	*In*
1–4	240	20	0.1	Lines
5–8	240	50	0.1	Lines
9–12	170	20	0.1	Lines
13–16	170	50	0.1	Lines
17–20	240	20	0.1	Wall
21–24	240	50	0.1	Wall
24–28	170	20	0.1	Wall

4 Results and discussion

Based on the description of the developed methodology, the ANN architecture of the case used for validating the approach is characterised by the structure reported in Figure 3. All the dimensions and the geometrical characteristics indicated in the input layer are referred to *GP*. On the other side, the output layer identifies the elements that the operators want to forecast to be sure that the white part respects the dimensions reported in the CAD. Since the parts considered for the analysis have a simple geometry and no external boundaries are imposed, it was assumed a tolerance equal to ±0.1 mm, which corresponds to the layer thickness used in the printing process. The data obtained by the CMM measuring the *GPs* are elaborated by the ANN and the predictions of the geometrical characteristics of the *WP* are obtained. In the meantime, the *GP* undergo to debinding and sintering process for obtaining the white part necessary for conducting the comparison of the experimental and predicted results. Then, the *WP* is measured for obtaining the actual data relative to the dimensions and geometrical characteristics.

The ANN predicts the shrinkages, and for comparing the data the final dimension is calculated reducing the *GP* measurements. The correspondence between the experimental and predicted data is shown in Figure 4. Nominal values (CAD) and the relatives upper and lower bounds (±0.1 for Figure 4 are reported. Two examples are reported taking into account one dimension that extends horizontally and one dimension that extends vertically. This differentiation is considered, since, as is reported in Quarto et al. (2021), the shrinkages that the metal-MEX parts show along X and Y directions are lower than the one along the Z direction. This aspect can be correlated to the effect of gravity that squashes the layers down during the printing phase increasing the shrinkage effect; indeed, it is demonstrated that along X and Y directions, the shrinkage is on average around 16%, whilst along Z-axis it is around 20%. The predictions fit well with the experimental data and, comparing the results it is estimated an average error in the prevision equals about 0.70%, varying in an interval between 0.01% and 3.32%. The error is very low indicating high reliability of the prediction demonstrating that the ANN is well-trained

Figure 4 Comparison between predicted and experimental results in terms of dimension along x-direction (left), along z-direction (right) (see online version for colours)

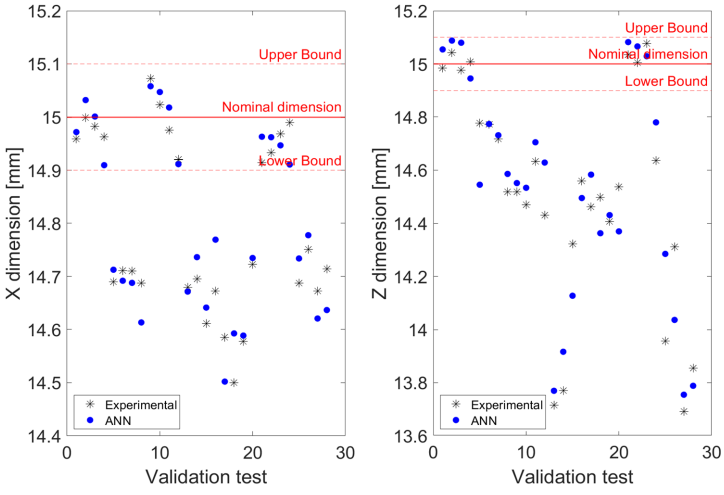

Regarding the density interval, the nominal value (it corresponds to the density of the rough material – stainless steel 316L) is considered also as upper bound. The lower bound is defined considering the historical data of the previous studies conducted by the authors (Quarto et al., 2021; Carminati et al., 2022). These studies show that the printed parts do not reach the same value as rough material and, usually, it is lower than the density declared in the material datasheet (7.8 kg/m^3). Such as evident from previous works and also from Figure 5, the density results in the most critical issues, since is characterised by higher variability in relation to the printing parameters.

Figure 5 Comparison between predicted and experimental results in terms of material density (see online version for colours)

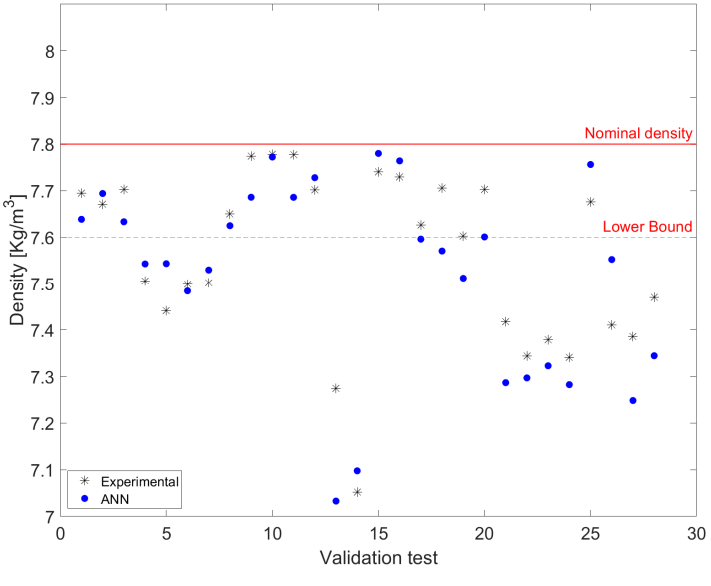

The definition of non-compliant parts is not immediate, since in some cases, not all the indicators are placed in the accepted interval. Thus, can be useful to cross-reference the collected data (both predicted and experimental) for answering to two main questions:

1 Is there a correspondence between the predicted and the experimental non-compliant parts?

2 Which parts are compliant considering all the parameters and constraints?

It is possible to answer these questions by means of Figures 6–8 where an example of the deviation (Δ) of the predicted and experimental compared to the nominals and the confidence interval is highlighted (green area) is reported. The radar representation allows identifying, for ANN and experiments, which parts can be considered as compliant reporting all the characteristics together. Comparing the two figures, the parts that would be discarded considering the predictive approach coincide with those that would also be considered non-compliant experimentally.

Figure 6 Identification of compliant and non-compliant parts by ANN approach as a function of dimension (see online version for colours)

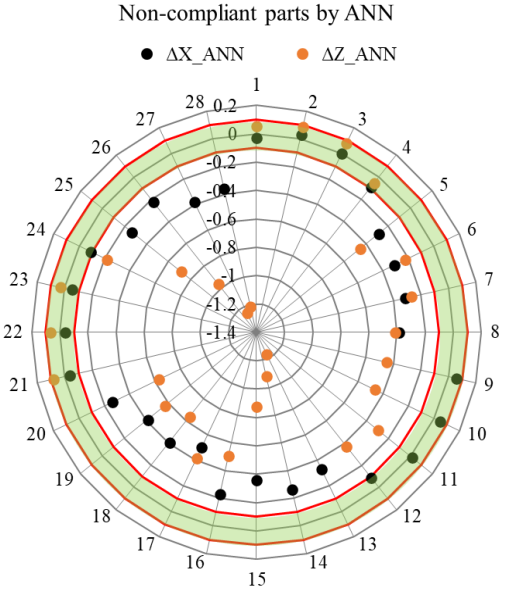

Supposing that all the outputs have the same importance from the design specification and for the functionality of the product, cross-referencing the results reported in Figures 6–8, for example, samples from 1 to 3 satisfy all the requirements, and without any doubt, they can be considered as compliant parts. For the other samples, there is a correspondence between the response for experimental and predicted data, but not all the requirements are satisfied.

Figure 7 Identification of compliant and non-compliant parts by experiments approach as a function of dimension (see online version for colours)

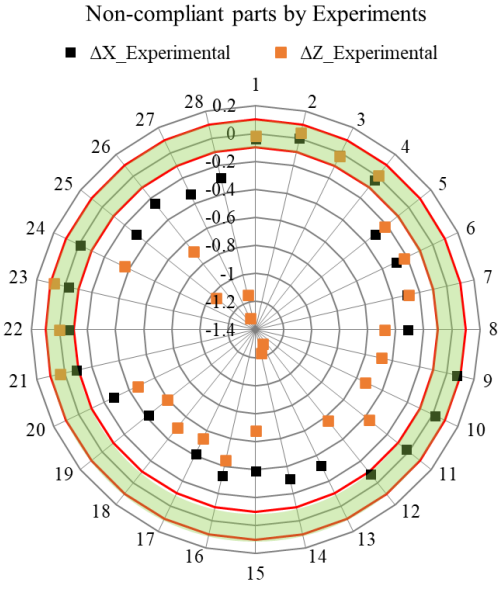

Figure 8 Identification of compliant and non-compliant parts as a function of density (see online version for colours)

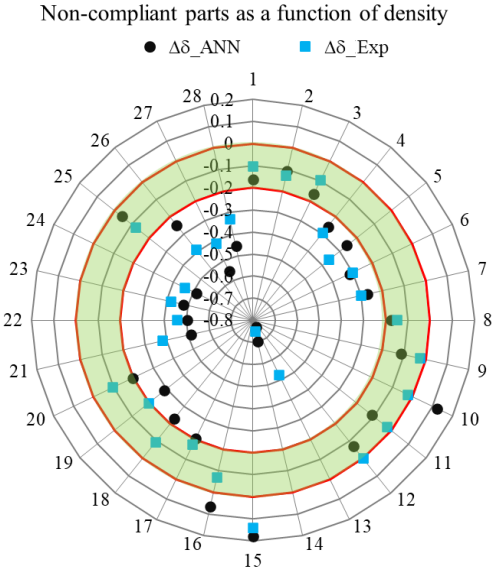

5 Conclusions

In this work, an approach for the detection of non-compliant parts in the middle of the manufacturing chain of the metal-MEX process was defined. First, the quality evaluation

was introduced immediately after the printing phase for having the chance of selecting, for the debinding and sintering process, only the green parts that result be promising in terms of compliance with the requirements. The approach is based on the introduction of a trained ANN able to predict the dimensions and/or geometrical characteristics of the white parts. The introduction of the skimming system before the execution of the post-printing processes allows reducing waste detected at the end of the production chain. In this way, it is possible both to reduce costs, since only the green parts that will almost certainly assume the required characteristics are subjected to treatments, and to anticipate any reproduction of the parts necessary to complete an order without having to oversize the production batches a priori.

The results show that the ANN is successfully trained, and the predicted results fit well with the experimental data demonstrating the ability of this algorithm to detect future non-compliant parts. The prediction error lies in a range between 0.01% and 3.32% demonstrating the effectiveness of the ANN training and the reliability of the approach. Furthermore, it is possible to cross-reference the results obtaining the evaluation of each green part as a function of several different indicators assigning different importance to them as a function of the design and customer requirements.

This work develops the algorithm defining the first steps for future integration in the industrial system for obtaining automatic response after the collection of the green parts measures. Considering the aspects of Quality 4.0, this approach can satisfy the requirements of control automation and prevention of defects; furthermore, the identification of the non-compliant parts before the binding and sintering processes allows the recycling of waste (material containing polymer and metal powder) to produce new filaments.

References

Al-Ahmari, A., Ashfaq, M., Mian, S.H. and Ameen, W. (2019) 'Evaluation of additive manufacturing technologies for dimensional and geometric accuracy', *Int J. Mater Prod Technol*., Vol. 58, pp.129–154, https://doi.org/10.1504/IJMPT.2019.097665

Baumgartl, H., Tomas, J., Buettner, R. and Merkel, M. (2020) 'A deep learning-based model for defect detection in laser-powder bed fusion using in-situ thermographic monitoring', *Prog Addit Manuf*., Vol. 5, pp.277–285, https://doi.org/10.1007/s40964-019-00108-3

Boschetto, A. and Bottini, L. (2014) 'Accuracy prediction in fused deposition modeling', *Int. J. Adv Manuf Technol.*, Vol. 73, pp.913–928, https://doi.org/10.1007/S00170-014-5886-4/METRICS

Bounds, D.G., Lloyd, P.J., Mathew, B. and Waddell, G. (1988) *Multi Layer Perceptron Network for the Diagnosis of Low Back Pain*, Publ by IEEE, Vol. 8, pp.481–489, https://doi.org/10.1109/icnn.1988.23963

Brøtan, V. (2014) 'A new method for determining and improving the accuracy of a powder bed additive manufacturing machine', *Int J. Adv Manuf Technol*., Vol. 74, pp.1187–1195, https://doi.org/10.1007/s00170-014-6012-3

Byun, H.S. and Lee, K.H. (2003) 'Design of a new test part for benchmarking the accuracy and surface finish of rapid prototyping processes', *Lect Notes Comput Sci (Including Subser Lect Notes Artif Intell Lect Notes Bioinformatics)*, Vol. 2669, pp.731–740, https://doi.org/10.1007/3-540-44842-X_74/Cover

Carminati, M., Quarto, M., D'Urso, G., Giardini, C. and Maccarini, G. (2022) 'Mechanical characterization of AISI 316L samples printed using material extrusion', *Appl. Sci.*, Vol. 12, p.1433, https://doi.org/10.3390/app.12031433

Chen, Y., Ding, Y., Zhao, F., Zhang, E., Wu, Z. and Shao, L. (2021) 'Surface defect detection methods for industrial products: a review', *Appl Sci*., Vol. 11, p.7657, https://doi.org/10.3390/app.11167657

Cybenko, G. (1988) *Continuous Valued Neural Networks with Two Hidden Layers are Sufficient*, Department of Computer Science, Trfts Univ.

Cybenko, G. (1989) 'Approximation by superpositions of a sigmoidal function', *Math Control Signals, Syst*., Vol. 2, pp.303–314, https://doi.org/10.1007/BF02551274

Czimmermann, T., Ciuti, G., Milazzo, M., Chiurazzi, M., Roccella, S., Oddo, C.M. and Dario, P. (2020) 'Visual-based defect detection and classification approaches for industrial applications–a survey', *Sensors (Switzerland)*, p.20, https://doi.org/10.3390/s20051459

Fera, M., Fruggiero, F., Lambiase, A. and Macchiaroli, R. (2016) 'State of the art of additive manufacturing: Review for tolerances, mechanical resistance and production costs', *Cogent Eng*., Vol. 3, p.1261503, https://doi.org/10.1080/23311916.2016.1261503

Ferreira, J.C., Alves, N.M.F. and Bártolo, P.J.S. (2004) 'Rapid manufacturing of medical prostheses', *Int J. Manuf Technol Manag*., Vol. 6, pp.567–583, https://doi.org/10.1504/IJMTM.2004.005940

Fischer, M. and Schöppner, V. (2014) 'Finishing of ABS-m30 parts manufactured with fused deposition modeling with focus on dimensional accuracy', *25th Annu Int Solid Free Fabr Symp &#65533; An Addit Manuf Conf SFF. 2014*, Austin (Texas), pp.923–934.

Garcia-Romeu, M.L., Ceretti, E., Fiorentino, A. and Giardini, C. (2010) 'Forming force prediction in two point incremental forming using backpropagation neural networks in combination with genetic algorithms', *ASME 2010 Int. Manuf. Sci. Eng. Conf. MSEC 2010*, Vol. 2, pp.99–106, https://doi.org/10.1115/MSEC2010-34142

Giganto, S., Martínez-Pellitero, S., Cuesta, E., Zapico, P. and Barreiro, J. (2022) 'Proposal of design rules for improving the accuracy of selective laser melting (SLM) manufacturing using benchmarks parts', *Rapid Prototyp J*, Vol. 28, pp.1129–1143, https://doi.org/10.1108/RPJ-06-2021-0130

Giudice, F., Barbagallo, R. and Fargione, G. (2021) 'A design for additive manufacturing approach based on process energy efficiency: electron beam melted components', *J. Clean Prod.*, Vol. 290, p.290, https://doi.org/10.1016/j.jclepro.2020.125185

Gregorian, A., Elliot, B. and Navarro, R. (2001) 'Accuracy improvement in rapid prototyping machine (FDM-1650)', *2001 Int Solid Free Fabr Symp*., Austin (Texas), Vol. 2001, pp.77–84.

Hecht-Nielsen, R. and Kolmogorov, S. (1987) *Mapping Neural Network Existence Theorem*, SOS Printing.

Ibrahim, M.S., Fan, J., Yung, W.K.C., Prisacaru, A., van Driel, W., Fan, X. and Zhang, G. (2020) 'Machine learning and digital twin driven diagnostics and prognostics of light-emitting diodes', *Laser Photonics Rev*., Vol. 14, p.2000254, https://doi.org/10.1002/lpor.202000254

International Organization for Standarization (2021) ISO/ASTM 52900: 2021 Additive Manufacturing – General Principles – Fundamentals and Vocabulary.

Jarosz, K. and Özel, T. (2022) 'Machine learning approaches towards digital twin development for machining systems', *Int J. Mechatronics Manuf Syst.*, Vol. 15, pp.127–148, https://doi.org/10.1504/ijmms.2022.124922

Kordatos, I.D. and Benardos, P. (2022) 'Comparative analysis of machine learning algorithms for steel plate defect classification', *Int J. Mechatronics Manuf Syst*., Vol. 15, pp.246–263, https://doi.org/10.1504/IJMMS.2022.127211

Kruth, J.P., Leu, M.C. and Nakagawa, T. (1998) 'Progress in additive manufacturing and rapid prototyping', *CIRP Ann – Manuf Technol*., Vol. 47, pp.525–540, https://doi.org/10.1016/S0007-8506(07)63240-5

Levy, G.N., Schindel, R. and Kruth, J.P. (2003) 'Rapid manufacturing and rapid tooling with layer manufacturing (LM) technologies, state of the art and future perspectives', *CIRP Ann – Manuf Technol*., Vol. 52, pp.589–609, https://doi.org/10.1016/S0007-8506(07)60206-6

Lieneke, T., Adam, G.A.O., Leuders, S., Knoop, F., Josupeit, S., Delfs, P., Funke, N. and Zimmer, D. (2020) 'Systematical determination of tolerances for additive manufacturing by measuring linear dimensions', *Proc. -26th Annu. Int. Solid Free. Fabr. Symp. -An Addit. Manuf. Conf. SFF. 2015*, Austin (Texas), pp.371–84.

Lieneke T., Denzer, V., Adam, G.A.O. and Zimmer D. (2016) NC-ND license (http://creativecommons.org/licenses/by-nc-nd/4.0/), Peer-Review under Responsibility of the Dimensional Tolerances for Additive Manufacturing: Experimental Investigation for Fused Deposition Modeling 2016, https://doi.org/10.1016/j.procir.2016.02.361.

Lippmann, R.P. (1987) 'An introduction to computing with neural nets', *IEEE ASSP Mag.*, Vol. 4, pp.4–22, https://doi.org/10.1109/MASSP.1987.1165576

Liravi, F., Darleux, R. and Toyserkani, E. (2015) 'Nozzle dispensing additive manufacturing of polysiloxane: dimensional control', *Int J. Rapid Manuf.*, Vol. 5, p.20, https://doi.org/10.1504/IJRAPIDM.2015.073546

López Rojas, A.D., Mendoza-Trejo, O., Padilla-García, E.A., Ortiz Morales, D., Cruz-Villar, C.A. and La Hera, P. (2022) 'Design, rapid manufacturing and modeling of a reduced-scale forwarder crane with closed kinematic chain', *Mech Based Des Struct Mach*., Vol. 14, No. 20, p.13092, https://doi.org/10.1080/15397734.2022.2063889

Majumder, A., Das, P.K., Majumder, A. and Debnath, M. (2014) 'An approach to optimize the edm process parameters using desirability-based multi-objective PSO', *Prod Manuf Res.*, Vol. 2, pp.228–240, https://doi.org/10.1080/21693277.2014.902341

Maren, A.J., Jones, D. and Franklin, S. (1990) 'Configuring and optimizing the back-propagation network', *Handb. Neural Comput. Appl.*, Elsevier, pp.233–250, https://doi.org/10.1016/b978-0-12-546090-3.50019-x

Meng, L., McWilliams, B., Jarosinski, W., Park, H.Y., Jung, Y.G., Lee, J. and Zhang, J. (2020) 'Machine learning in additive manufacturing: a review', *Jom*, Vol. 72, pp.2363–2377, https://doi.org/10.1007/s11837-020-04155-y

Papazetis, G. and Vosniakos, G.C. (2019) 'Mapping of deposition-stable and defect-free additive manufacturing via material extrusion from minimal experiments', *Int J. Adv Manuf Technol*., Vol. 100, pp.2207–2219, https://doi.org/10.1007/s00170-018-2820-1

Quarto, M. and Carminati, M. and D'Urso, G. (2021) 'Density and shrinkage evaluation of AISI 316L parts printed via FDM process', *Mater Manuf Process*, Vol. 36, pp.1535–1543, https://doi.org/10.1080/10426914.2021.1905830

Quarto, M., Bocchi, S., D'Urso, G. and Giardini, C. (2022) 'Hybrid finite elements method-artificial neural network approach for hardness prediction of AA6082 friction stir welded joints', *Int J. Mechatronics Manuf Syst.*, Vol. 15, pp.149–166, https://doi.org/10.1504/ijmms.2022.124919

Quarto, M., D'Urso, G. and Giardini, C. (2022) 'Micro-EDM optimization through particle swarm algorithm and artificial neural network', *Precis Eng.*, Vol. 3, pp.63–70, https://doi.org/10.1016/j.precisioneng.2021.08.018

Quarto, M., Giardini, C. (2022) 'Additive manufacturing of metal filament: when it can replace metal injection moulding', *Prog Addit Manuf.*, Vol. 8, pp.561–570, https://doi.org/10.1007/s40964-022-00348-w

Ryan, K.R., Down, M.P. and Banks, C.E. (2021) 'Future of additive manufacturing: overview of 4D and 3D printed smart and advanced materials and their applications', *Chem. Eng. J.*, Vol. 403, p.126162, https://doi.org/10.1016/j.cej.2020.126162

Sun, W., Starly, B., Nam, J. and Darling, A. (2005) 'Bio-CAD modeling and its applications in computer-aided tissue engineering', *CAD Comput Aided Des.*, Vol. 37, pp.1097–1114, https://doi.org/10.1016/J.CAD.2005.02.002

Westphal, E. and Seitz, H. (2021) 'A machine learning method for defect detection and visualization in selective laser sintering based on convolutional neural networks', *Addit Manuf.*, Vol. 41, p.101965, https://doi.org/10.1016/j.addma.2021.101965

Wiberg, A., Persson, J. and Ölvander, J. (2019) 'Design for additive manufacturing – a review of available design methods and software', *Rapid Prototyp, J*., Vol. 25, pp.1080–1094, https://doi.org/10.1108/RPJ-10-2018-0262

Wohlers, T., Campbell, R.I., Diegel, O., Kowen, J. and Ray Huff, N.M. (2021) *Wohlers Report 2021*, Wohlers Rep 2016, p.375.

Yadav, D., Chhabra, D., Kumar Garg, R., Ahlawat, A. and Phogat, A. (2020) 'Optimization of fdm 3D printing process parameters for multi-material using artificial neural network', *Mater Today Proc.*, Vol. 21, pp.1583–1591, https://doi.org/10.1016/j.matpr.2019.11.225

Yorulmuş, M.H., Bolat, H.B. and Bahadır, Ç. (2022) 'Predictive quality defect detection using machine learning algorithms: a case study from automobile industry', *Lect Notes Networks Syst*., Vol. 308, pp.263–270, https://doi.org/10.1007/978-3-030-85577-2_31